In Situ Optical Studies of Flow-Induced Orientation in a Two-Dimensional Polymer Solution

Matthew C. Friedenberg,† Gerald G. Fuller,* Curtis W. Frank, and Channing R. Robertson

Department of Chemical Engineering, Stanford University, Stanford, California 94305-5025

Received June 6, 1995; Revised Manuscript Received October 2, 1995[⊗]

ABSTRACT: The orientation dynamics of polymers in constrained geometries is considered through studies of monolayer films at the air−water interface. Here, *in situ* optical techniques are employed to probe flow orientation in monolayers of phthalocyaninatopolysiloxane dispersed in either docosanoic acid, 1,2-dimyristoyl-*sn*-glycero-3-phosphatidylcholine, or arachidyl alcohol. Compression of the polymer monolayer creates alignment perpendicular to the compression direction. A well-defined extensional flow is imposed in the monolayer to study the dynamics of flow-induced anisotropy. The orientation process obeys a strain-scaling law, indicating the absence of relaxation on the time scale of the flow.

Introduction

The Langmuir−Blodgett (LB) technique, in which ultrathin films are prepared by transferring monolayers from the air−water interface onto solid substrates, offers unique capabilities for the creation of supramolecular assemblies with a defined layer structure.[1] Films of rigid and semirigid polymers are of special interest for their high stability, nonlinear optical properties, and ability to function as alignment layers for liquid-crystal displays.[2] A key requirement for these applications is the manufacture of films with a high degree of orientational order. The extent to which the LB technique can produce such order depends on the material properties of the monolayer film and the types of processing to which it is subjected.

Films at the air−water interface can be transferred to solid substrates by a process known as vertical deposition, in which a substrate is dipped and withdrawn through the compressed monolayer; ideally transferring one monolayer onto the substrate for each upstroke and downstroke. For films of both rigid and flexible polymers, the deposition process often creates enhanced alignment of the polymer backbone parallel to the dipping direction. This effect has been observed by polarized spectroscopy and atomic force microscopy (AFM) of LB films in several polymer systems, including polyglutamates,[3] phthalocyanine polymers,[4,5] polysilanes,[6] polyimides,[7] and others.[8] In contrast, AFM studies of fatty acid LB films and their salts reveal that the degree of order in these films depends not on the processing of the film during deposition but on such equilibrium parameters as the structure of the substrate and the proximity of the film layer to the substrate.[9]

Thus, it is important to understand the fundamental interactions that control the development of molecular alignment during vertical deposition. Analyses of transferred films are not sufficient to accomplish this, since the deposited film structure represents the cumulative orientational effect of the entire deposition process. Moreover, the dynamics of the orientational phenomena, which define the characteristic time scales for molecular alignment and relaxation, are not accessible in studies of transferred films. To isolate the individual factors that contribute to the resulting order, studies must be conducted at the air−water interface. The influence of the deposition process on macroscopic domain structure has already been addressed through fluorescence microscopy studies at the three-phase contact line, where air, film, and substrate meet.[10] Fluorescence microscopy has also been used to directly visualize the flow of tetradecanoic and pentadecanoic acid domains through a channel.[11] A related topic, the effect of flow on the dynamics of domain-shape changes in lipid monolayers, is also an active area of study.[12]

In this article, we investigate the coupling of hydrodynamics to molecular orientation for monolayers on rodlike polymers dispersed in low molecular weight amphiphiles at the air−water interface. High-speed optical techniques are used to probe the orientational dynamics of the polymer molecules in response to an applied flow. We consider the orientational response of monolayers of phthalocyaninatopolysiloxane (PcPS), a hairy-rod polymer shown schematically in Figure 1. PcPS is a rigid polymer of cofacially stacked phthalocyanine rings joined by a polysiloxane backbone and grafted at the periphery with C_8 alkyl chains.[13] Because of its rodlike character, PcPS is found to align parallel to the dipping direction in LB films.[4,5]

The degree of molecular order in PcPS films can be determined from the anisotropy in the absorption of light by the floating monolayer. This leads to a linear dichroism, $\Delta n'' = n_1'' - n_2''$, in the sample, where n_1'' and n_2'' are the principal values of the imaginary part of the refractive index. PcPS has a strongly polarized absorption, with a maximum occurring when the electric field vector of the incident light is in the plane of the phthalocyanine ring. Since the polymer backbone lies parallel to the water surface[4] in monolayers, the absorption of polarized light by a PcPS monolayer becomes a strong function of the orientational distribution of the individual polymer molecules in the plane of the air−water interface. Schwiegk et al.[5] have demonstrated that PcPS absorption is strong enough to permit linear dichroism measurements in transferred monolayers. In the present study, the dichroism is measured dynamically by rapidly modulating the polarization of the light incident on the sample.[14] In addition to the dichroism, which is proportional to the scalar order parameter, the experiment independently yields the average angle of polymer orientation in the monolayer, χ, relative to a chosen laboratory axis.

* To whom all correspondence should be addressed.
† Present address: IBM Almaden Research Center, 650 Harry Road, K63/803, San Jose, CA 95120.
⊗ Abstract published in *Advance ACS Abstracts,* December 15, 1995.

0024-9297/96/2229-0705$12.00/0

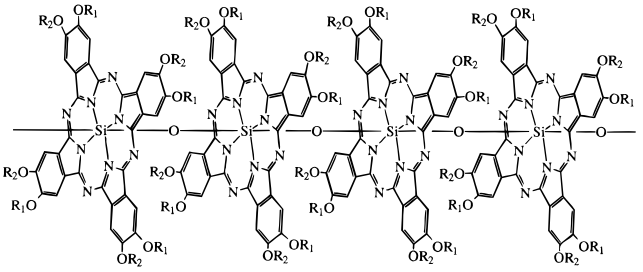

Figure 1. Chemical structure of phthalocyaninatopolysiloxane (PcPS). $R_1 = CH_3$, $R_2 = C_8H_{17}$.

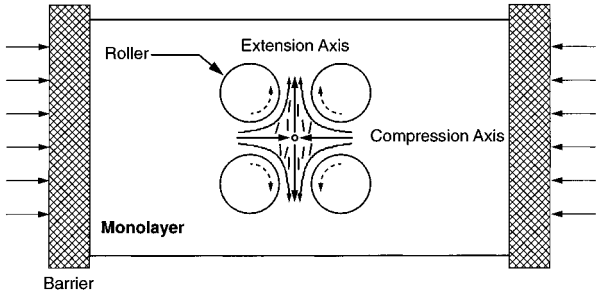

Figure 2. Schematic of the four-roll mill, top view, and resulting extensional flow field and molecular orientation. The monolayer is in the plane of the page. Dashed curves indicate the rotation direction of the rollers. Solid curves represent the hyperbolic streamlines characteristic of this flow. The small rods depict rodlike polymer molecules, greatly exaggerated in size, with the expected orientation parallel to the extension axis. The open circle at the center of the flow field represents the stagnation point, where the velocity of the monolayer is negligible.

It has been established that the vertical deposition process induces velocity gradients in a floating monolayer as it flows toward the substrate[15] and that these gradients can be correlated with the presence of orientational order in polymeric LB films.[5] Though the specific flow created by the deposition process is of obvious practical interest, it is a complex mix of shear and extension with deformation rates that vary from point to point. This spatial inhomogeneity complicates the analysis of the observed orientational dynamics. Thus, the present study uses a model flow field, created by a device known as a four-roll mill, to investigate these phenomena under well-defined conditions. The four-roll mill is a flow device invented by G. I. Taylor to study droplet deformation in emulsions.[16] This device, shown schematically in Figure 2, consists of four cylindrical rollers centered on the corners of a square. By varying the individual rate and direction of rotation of the four rollers, the amount of extension and rotation in the flow can be controlled.[17] If adjacent rollers are rotated at equal speeds and in opposite directions, a pure straining (extensional) deformation is produced in the monolayer that is homogeneous over a considerable portion of the area between the rollers. This extensional deformation can be characterized by a uniform strain rate, $\dot{\epsilon}$, which is directly proportional to the angular velocity of the rollers. The axis along which material enters the mill is the compression axis, and the axis along which it exits is the extension axis. In this kind of flow, elongated particles are known to align with their long axis parallel to the extension axis,[18] as shown in Figure 2. An important feature of this flow is the existence of a stagnation point at the center of the flow field, where residence times are long and therefore the material has the greatest opportunity to achieve a steady-state orientation.

Materials and Methods

PcPS. Samples of PcPS were generously donated by Dr. Andreas Ferencz and Professor Gerhard Wegner of the Max Planck Institute for Polymer Research in Mainz. Two molecular weights were investigated, PcPS Kurz and PcPS Ultra.[19] PcPS Kurz is the lower molecular weight sample, with a degree of polymerization of approximately 25. PcPS Ultra is the higher molecular weight preparation, with a degree of polymerization of approximately 50.

We have blended the polymer with short-chain amphiphiles to improve the flow behavior of the surface film. Three PcPS mixtures have been prepared for these studies: 5 mol % PcPS Kurz in docosanoic acid ($C_{21}H_{43}COOH$), 20 mol % PcPS Ultra in 1,2-dimyristoyl-*sn*-glycero-3-phosphatidylcholine (DMPC), and 5 mol % PcPS Ultra in arachidyl alcohol (molar concentrations have been calculated using the molecular weight of the PcPS monomer).

Monolayer Preparation. Monolayers were prepared in an 11 cm × 70 cm KSV 5000 alternate layer Langmuir−Blodgett trough equipped with a Wilhelmy balance for surface pressure measurement (KSV Instruments, Helsinki). The trough was placed on a vibration-isolation table (Technical Manufacturing Corp., Peabody, MA) equipped with "full perimeter enclosure", allowing optical and mechanical components to be mounted on a frame that was vibrationally isolated from the tabletop. A Milli-RO/Milli-Q system (Millipore) produced purified water with a resistivity of 18.2 MΩ cm^{-1}. All experiments were performed at 25.0 ± 0.2 °C and a pH of 5.6 ± 0.1. Monolayers were compressed at a rate of 1.1 $Å^2$/(molecule min) to a surface pressure of 20 mN/m and held at this pressure for 15 min prior to initiation of flow.

Four-Roll Mill. The rollers of the four-roll mill were constructed from black Delrin. The diameter of the rollers was 0.781 in., the length 2.0 in., and the distance between adjacent rollers 1.25 in. It was recently shown that this ratio of roller diameter to roller spacing, 0.625, provided the closest approximation to homogeneous extension for bulk flows.[20] A Compumotor stepping motor (Model M57-51) and indexer (Model 3000) were used to drive the rotation of the rollers, which were geared together to facilitate the production of extensional flow. Measurements of film area at constant surface pressure, in the absence and presence of flow, indicated that the flow did not cause any area loss in the monolayer. Control isotherms confirmed that the Delrin rollers did not contaminate the water surface.

The four-roll mill was immersed in the Langmuir−Blodgett trough to a depth of approximately 1 in. and positioned so that the compression and extension axes of the flow were parallel and orthogonal to the moving barriers, respectively. The compression and extension axes could be interchanged by reversing the direction of roller rotation.

Flow Visualization. A particle tracking method was used to visualize the flow of monolayer films in response to an applied extensional deformation. Monolayers were first compressed to the desired surface pressure and then seeded with sulfur powder.[21] The films were illuminated from the front side with a 40 W light bulb, and the motion of the sulfur particles were recorded with a CCD camera (Sanyo VDC3825) mounted directly above the monolayer. The video output of the camera was connected to a SVHS VCR (Panasonic AG1975). Flow visualization images were digitized with a PC frame grabber (Data Translation DT3851-8) and processed using Global Lab Image software (Data Translation) to determine the particle trajectories.

Polarization-Modulated Linear Dichroism. A description and analysis of the optical train used in these studies has been discussed previously.[22] A similar apparatus, used in a scanning mode, has recently been developed by another laboratory to investigate molecular order in transferred multilayers.[19] In our instrument, the intensity of light (543.6 nm green He−Ne) transmitted through the monolayer is measured with a photodiode submerged in the trough. This photodiode is mounted in a watertight housing constructed entirely of fluorocarbon polymers, to avoid contamination of the water, and the electrical signal is passed out of the water through

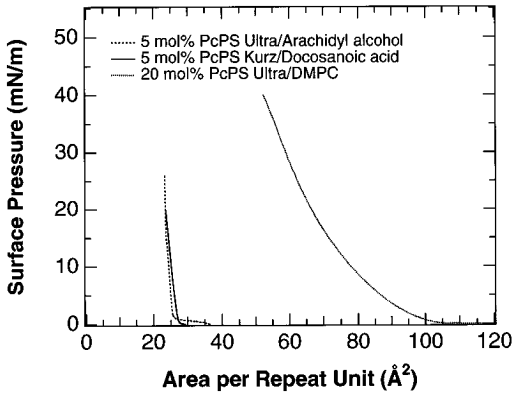

Figure 3. Pressure−area diagrams for the three PcPS mixed monolayers used in these studies.

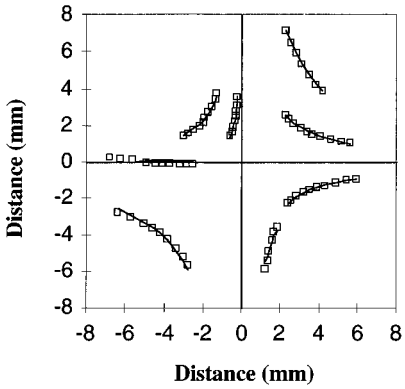

Figure 4. Sulfur particle trajectories and best-fit hyperbolic streamlines for 5% PcPS Ultra/arachidyl alcohol monolayers, 30 mN/m, roller velocity = 0.11 revolutions/s.

the unused trough of our dual-trough instrument. This allowed the intensity signal to be measured without disturbing the flow of the monolayer. In reporting the experimental results, we express the dichroism as an anisotropy parameter, $\delta'' = (2\pi\Delta n'' d)/\lambda$, where d is the thickness of the monolayer film and λ is the wavelength of the incident light. We defined the laboratory coordinate system so that an angle of 0° corresponds to alignment of the rodlike polymer backbone parallel to the direction of monolayer compression (perpendicular to the barriers).

Results and Discussion

Pressure−Area Diagrams. The pressure−area diagrams for the three PcPS mixtures are shown in Figure 3. The isotherms are graphed in terms of an "area per repeat unit", where one repeat unit represents one monomeric unit of the phthalocyanine polymer or one molecule of the fatty acid/fatty alcohol/phospholipid matrix. Both the PcPS Ultra/arachidyl alcohol and PcPS Kurz/docosanoic acid films exhibit condensed phases at room temperature. As evidenced by the steep slope of the pressure−area diagram, these films have low compressibilities. In contrast, PcPS Ultra/DMPC forms an expanded monolayer at room temperature, with a more gradual rise in surface pressure during compression.

Flow Behavior of PcPS Monolayers. We have used a particle tracking method to provide a qualitative description of the flow behavior of PcPS monolayers. These studies indicate that the response to an applied deformation can depend quite strongly on the monolayer composition. For example, a pure PcPS monolayer is too rigid to flow when the rollers of the four-roll mill are rotated. The monolayer will flow if the polymer is mixed into a matrix of docosanoic acid at moderate concentrations, but the response is then dominated by the flow of solidlike islands rather than a fluid continuum. This island flow is diminished as the polymer concentration is reduced. The use of a less viscous matrix, such as DMPC, can lead to a flow response dominated by inertial effects, in which the monolayer continues to track the initial streamlines for a short time even after the flow direction is reversed. All of these flow effects are important in determining the orientational response of a specific monolayer film to flow. This behavior can be described by the Reynolds number,[23] which characterizes the balance of inertial forces to viscous forces in the film. At high strain rates or low surface viscosities, the Reynolds number is greater than unity, and inertial effects will dominate the observed flow behavior. At low strain rates and high surface viscosities, the Reynolds number is less than unity, and only the viscous effects will be important. Other films may exhibit solidlike behavior, exhibiting yield stresses and brittle failure. Therefore, the physical properties of the monolayer are critically important in determining the orientational response of a specific monolayer film to an applied deformation.

Characterization of the Extensional Flow Field. To characterize the extensional flow generated by the four-roll mill, we performed a quantitative analysis of the flow visualization images. This allowed determination of the functional relationship between the angular velocity of the rollers and the strain rate of the flow field. Here we present results for monolayers of 5 mol % PcPS Ultra in arachidyl alcohol at a surface pressure of 30 mN/m.

Figure 4 shows the sulfur particle trajectories when the rollers of the four-roll mill are rotated at 0.11 revolutions/s. This graph was generated from video images of the sulfur particles, digitized at a frequency of 1 frame/s. The symbols represent the center of mass of the sulfur particles, and the solid curves correspond to the best-fit hyperbolic streamlines through these coordinates. The agreement between the actual and ideal streamlines is very good, indicating that the mill imposes a close approximation to a planar extensional flow in the monolayer. Errors from the finite size of the sulfur particles should be most significant near the compression and extension axes, where the streamlines are close together; thus, the less adequate fit for the streamline on the negative horizontal axis is not surprising.

These trajectories can be used to calculate the strain rate of the extensional flow field. The velocity gradient tensor produced by the four-roll mill, $\mathbf{\Gamma} = \nabla\mathbf{v}$, can be written in two dimensions as

$$\mathbf{\Gamma} = \begin{bmatrix} \dot{\epsilon} & 0 \\ 0 & -\dot{\epsilon} \end{bmatrix} \tag{1}$$

where $\dot{\epsilon}$ is the strain rate. The streamlines of this flow are hyperbolic and can be written as

$$\frac{dx}{dt} = \dot{\epsilon}x \tag{2}$$

$$\frac{dy}{dt} = -\dot{\epsilon}y \tag{3}$$

Integrating the expressions for the x and y components of the extensional flow streamlines (eqs 2 and 3) yields the following idealized trajectories for the sulfur particles:

$$\frac{x}{x_0} = \exp(\dot{\epsilon}t) \tag{4}$$

$$\frac{y}{y_0} = \exp(-\dot{\epsilon}t) \tag{5}$$

where (x_0, y_0) represents the particle coordinates at some initial time $t = 0$. From these equations, it is evident that a graph of $\ln(x/x_0)$ or $-\ln(y/y_0)$ versus time should be linear, with slope $\dot{\epsilon}$. We have calculated the strain rate for each particle path and averaged these together to obtain a mean value.

In Figure 5, the mean strain rate determined by the above procedure is graphed against roller velocity for monolayers of 5 mol % PcPS Ultra in arachidyl alcohol at 30 mN/m. As expected, the relationship between the roller velocity and strain rate is linear. This calibration curve is not universal, however, as we have found that the correlation depends on both the composition of the monolayer and the size of the four-roll mill.

Compression-Induced Orientation. It is of interest to consider the molecular orientation that develops during preparation of the monolayer at the air−water interface, since the compression process is known to establish velocity gradients in the floating monolayer.[5,15] In Figure 6, the surface pressure, π, optical anisotropy, δ'', and average orientation angle, χ, are graphed as a function of molecular area during continuous compression of a monolayer of 5 mol % PcPS Kurz in docosanoic acid. The measured anisotropy suggests that the PcPS molecules undergo a transition, coincident with the initial rise in surface pressure, from a disordered state to an ordered one. This order is enhanced after further compression. Moreover, the average orientation angle approaches 90°, corresponding to a net orientation of the polymer backbone perpendicular to the direction of compression. Although compression-induced alignment has been observed in other monolayer systems under static conditions,[21,24] the techniques employed here allow dynamic measurement of optical anisotropy, orientation angle, and surface pressure during monolayer compression. We note that the fluctuations observed in the optical signals reported here are always small compared with the specific response to the applied deformation.

Extensional Flow-Induced Orientation. Since the ordering induced by compression is sensitive to strain history and relaxes slowly, the monolayer is not in a reproducible initial state after compression. To create a consistent starting point for the extensional flow studies, the compressed monolayer is first prestrained with the four-roll mill until the optical anisotropy approaches a steady state. Then, to probe the orientational response of the monolayer, the flow direction is reversed by rotating the rollers of the mill in the opposite direction. In Figure 7, the optical anisotropy (Figure 7a) and orientation angle (Figure 7b) are shown as a function of time for a reversal in the flow direction. These data are for a monolayer of 5 mol % PcPS Ultra in arachidyl alcohol ($\dot{\epsilon} = 0.05$ s^{-1}), but the behavior is similar in the docosanoic acid and DMPC matrices. Before the flow is reversed, the extinction fluctuates slightly around a mean value, and the orientation angle indicates that the PcPS molecules are aligned along the extension axis at 0°. After flow reversal, the extinction first decreases to nearly zero and then increases to a steady-state value. The average orientation angle switches by 90° at the point where the optical anisotropy

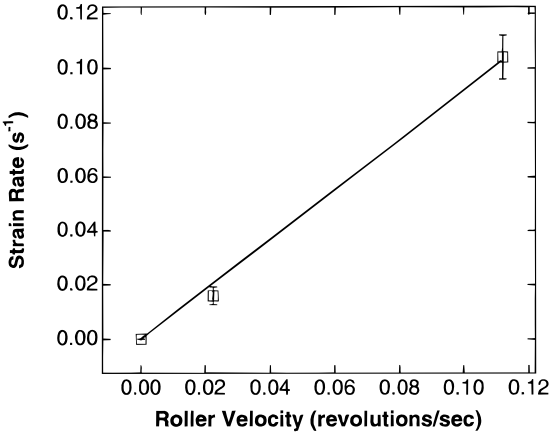

Figure 5. Relationship between roller velocity and observed strain rate for monolayers of 5 mol % PcPS Ultra in arachidyl alcohol.

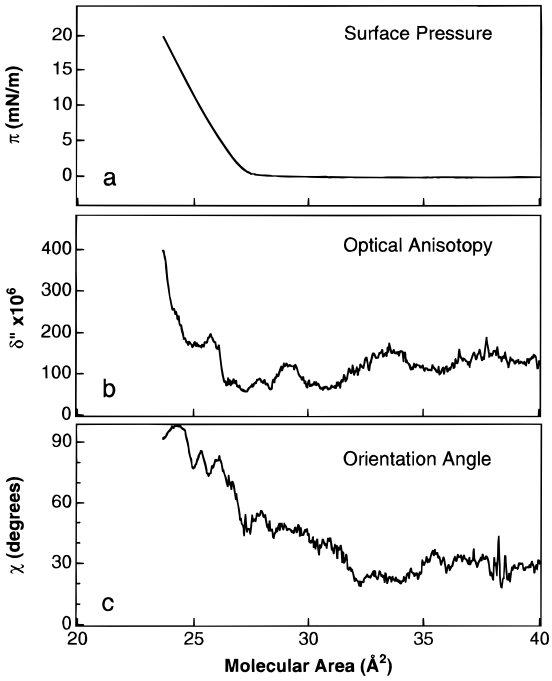

Figure 6. Compression-induced orientation in 5 mol % PcPS Kurz/docosanoic acid monolayers. (a) Surface pressure, (b) optical anisotropy, and (c) orientation angle measured as a function of the average area per molecule during continuous compression of the monolayer film.

passes through a minimum. This is an important confirmation of the quality of the applied extensional flow, since the symmetry of the mill dictates that the molecules should only align at 0 or 90°. Therefore, the applied extensional flow couples to the molecular orientation of PcPS, causing flow alignment along the extension axis. The dynamics of this process are discussed in a later section.

Influence of Surface Pressure on Steady-State Anisotropy. In Figure 8, the dependence of the steady-state anisotropy on surface pressure is shown for two systems: 5 mol % PcPS Ultra in arachidyl alcohol and 20 mol % PcPS Ultra in DMPC. These molar concentrations were chosen to provide similar area fractions of polymer, since DMPC forms significantly more expanded monolayers than arachidyl alcohol. For the PcPS/arachidyl alcohol monolayer, the dependence on surface pressure is very weak, with a slight increasing trend at higher surface pressures. In contrast, the

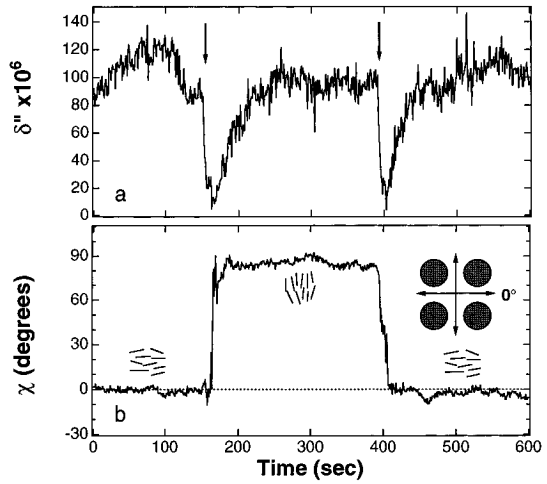

Figure 7. Orientational response of 5 mol % PcPS Ultra/arachidyl alcohol to an extensional flow reversal (30 mN/m). The monolayer was prestrained with the extension axis at 90° prior to these measurements. The optical anisotropy (a) and orientation angle (b) are reported through two reversals in the flow direction.

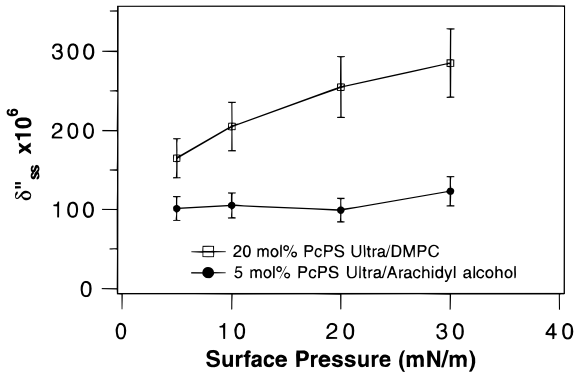

Figure 8. Surface pressure dependence of the steady-state anisotropy for PcPS Ultra in DMPC and arachidyl alcohol matrices.

PcPS/DMPC monolayer shows a strong increase in dichroism as the surface pressure increases. These results are correlated with the compressibilities of the matrix molecules, which is related to the slope of the pressure−area diagrams in Figure 3. DMPC monolayers exist in an expanded phase throughout the entire surface pressure range and are therefore highly compressible. The area concentration of polymer is thus enriched as the monolayer is compressed, leading to enhanced absorption. Arachidyl alcohol monolayers, however, form only condensed phases under the experimental conditions used here, and the pressure−area diagram for this molecule is nearly vertical. Therefore, the area concentration of polymer does not vary significantly over this range of surface pressure for the condensed monolayer.

Influence of Strain Rate on Steady-State Anisotropy. We studied the influence of strain rate on the steady-state anisotropy for monolayers containing 5 mol % PcPS Ultra in arachidyl alcohol. Five strain rates were investigated, from 0 to 0.10 s^{-1}. The protocol was as follows: The monolayer was prestrained at 0.1 s^{-1} for about 3 min to obtain a reproducible initial condition. The flow direction was then reversed by rotating the rollers in the opposite direction at the same speed. When the anisotropy reached a steady state, the strain rate was decreased to 0.02 s^{-1}. The anisotropy was again allowed to reach a steady state, and the strain rate was decreased further. This process continued for all five strain rates.

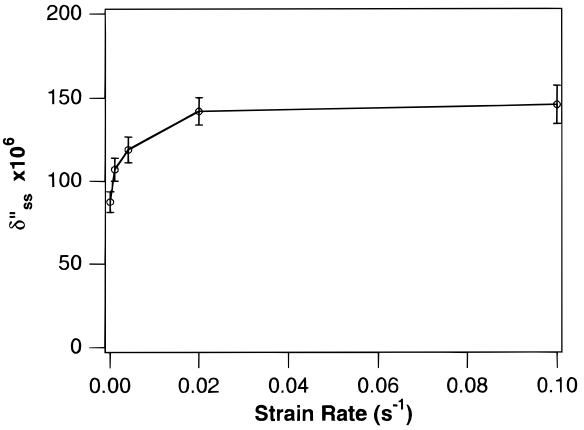

Figure 9. Dependence of the steady-state extinction on strain rate for a 5 mol % PcPS/arachidyl alcohol monolayer (30 mN/m).

The strain rate dependence of the steady-state anisotropy is shown in Figure 9. The anisotropy is independent of strain rate above 0.02 s^{-1}, suggesting that the rodlike polymer molecules have completely aligned in the flow field. This corresponds to values of the Deborah number, *De*, much greater than unity, where *De* is a dimensionless group defined as the ratio of the relaxation time scale of the monolayer to the characteristic time scale of the flow.[25] Here, we define the characteristic time scale of the flow as the reciprocal of the strain rate. Similar degrees of alignment by extensional flow have been reported in bulk studies of rigid-rod polymer solutions.[26] Below 0.02 s^{-1}, the ansiotropy decreases as the flow becomes weaker. Clearly, the flow is competing with some relaxation process over this time scale ($De = O(1)$). Since the anisotropy does not vanish, even after the flow is stopped, the flow-aligned polymer rods must remain ordered at rest. This may indicate the presence of nematic-like order in the monolayer, in which rotational diffusion is balanced by a thermodynamic potential. Alternatively, the monolayer may remain ordered for kinetic reasons, which would be the case if the rotational diffusivity of the polymer is so small that the orientation becomes effectively "frozen in". This issue is revisited below.

Flow-Reversal Dynamics. One of the most powerful features of the polarization-modulation linear dichroism technique is its ability to probe the dynamics of orientational phenomena in real time. These dynamics provide important information about the relative magnitudes and time scales of competing interactions that define the flow response in a given monolayer system.

The dynamics of PcPS orientation in response to a reversal in the extensional flow direction are presented in Figure 10. We investigated strain rates between 0.01 and 0.1 s^{-1}, corresponding to the plateau region in Figure 9. In these experiments, the monolayer was prestrained with the extension axis at 90° until a steady state was reached. Then, at zero time, the flow direction was reversed, and the orientational dynamics were measured until a new steady state was achieved. Since the average orientation angle is restricted to either 0 or 90° in flow, we incorporated this angular information into the sign of the optical anisotropy by multiplying the anisotropy by $\cos(2\chi)$. Here, negative values of this product correspond to a backbone orientation of 90°, and positive values represent alignment at 0°. As expected,

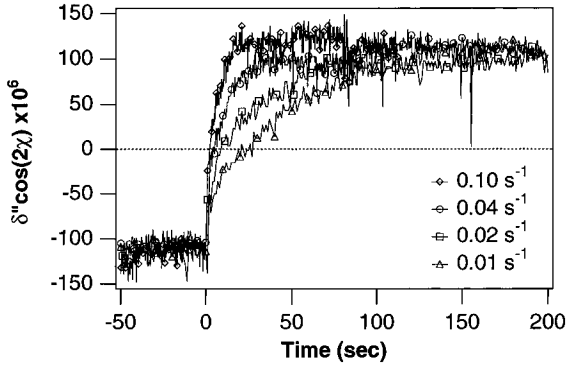

Figure 10. Flow-orientation dynamics as a function of strain rate for a monolayer containing 5 mol % PcPS Ultra in arachidyl alcohol (30 mN/m).

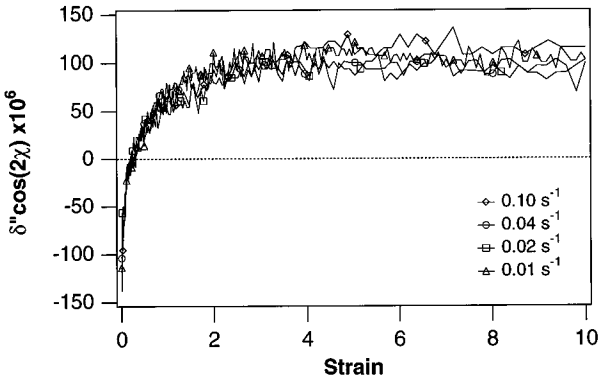

Figure 11. Strain scaling of flow-orientation dynamics for monolayers of 5 mol % PcPS Ultra in arachidyl alcohol.

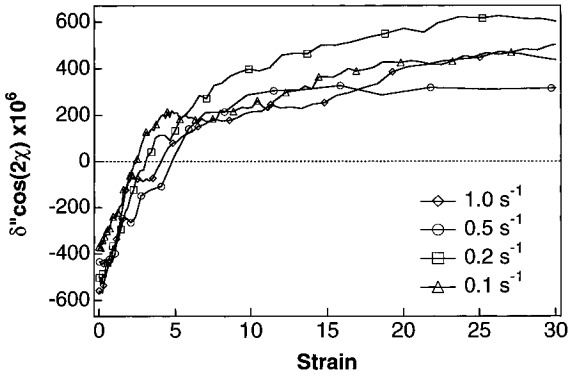

Figure 12. Flow orientation in monolayers of 5 mol % PcPS Kurz in docosanoic acid as a function of total strain (20 mN/m).

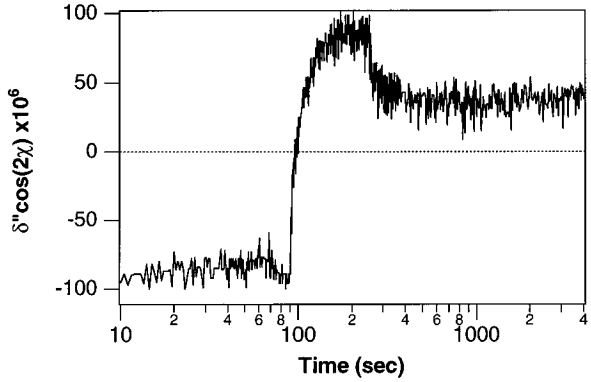

Figure 13. Relaxation of anisotropy following cessation of flow for monolayers of 5 mol % PcPS Ultra/arachidyl alcohol.

the time scale of the molecular orientation becomes faster as the strain rate increases.

In Figure 11, these transient orientation data are graphed against the total strain that the monolayer has experienced since the time of the flow reversal. In the extensional flow geometry described here, the total strain increases exponentially with the product of strain rate and time. The traces for all four strain rates superpose when graphed in terms of strain, signifying that the orientational response of the monolayer scales with total strain. Therefore, on the time scale of the flow, the coupling of the extensional flow to polymer orientation is the only significant contribution to the optical response. Strain scaling has also been observed in bulk studies of polymer liquid crystals during flow,[22] though not exclusively.[27]

We observed a qualitatively similar transient response in preliminary flow-orientation studies of 5% PcPS Kurz in docosanoic acid. These studies were performed on a smaller version of the four-roll mill (roller diameter = 0.484 in., spacing = 0.625 in.), and the extensional flow was created by manual rotation of the rollers. The flow-orientation data for this system, graphed as a function of total strain, are shown in Figure 12. Although the noise is greater in this system, the trend of strain scaling is clear. Steady state is reached at approximately 15 strain units, compared to 3 strain units for PcPS Ultra in arachidyl alcohol. This disparity arises from the presence of a rapid orientational relaxation in the latter system, discussed below. The difference in the magnitude of the steady-state extinction for these systems may arise from local compositional variations.

Relaxation. The strain-rate dependence of the steady-state anisotropy for the 5% PcPS Ultra/arachidyl alcohol system (Figure 9) indicates that the applied extensional flow competes with an orientational relaxation at strain rates below 0.02 s^{-1}. The time scale of this relaxation can be approximated by the reciprocal of this strain rate, or 50 s. In Figure 13, this orientational relaxation is directly investigated by following the decrease in optical anisotropy after flow cessation. For times less than 90 s, the monolayer is subjected to an extensional flow (strain rate = 0.04 s^{-1}) with the extension axis and polymer orientation at 90°. After 90 s, the rotation direction of the rollers is reversed, and the PcPS reorients parallel to the new extension axis. After 250 s, the extensional flow is stopped. Following the cessation of flow, there is a rapid initial relaxation during which the anisotropy decreases by 50−60%. After this, the anisotropy remains essentially constant for 3 h. An analysis of the time scale of this initial relaxation, obtained by a single-exponential fit, yields a relaxation time of approximately 20 s, in good agreement with that calculated from Figure 9.

The mechanism of this relaxation is currently unknown. One hypothesis is that it represents a rapid equilibration between the rotational diffusion of the polymer and the nematic potential of the polymer rods. Alternatively, the initial relaxation may be an elastic effect, in which stored energy is released following flow cessation. Visualization of the monolayer with sulfur particles supports this latter hypothesis, since we observe a significant macroscopic backflow following the cessation of flow. This backflow occurs over the same time scale as the orientational relaxation.

Modeling. To model the orientational dynamics observed with linear dichroism, we have used a statistical approach developed for bulk polymer liquid crystal rheology. Marrucci and Maffettone[28] proposed a two-

dimensional model to describe the flow behavior of polymer liquid crystals in shear. This model is a dimensionally constrained version of a theory by Doi[29] that describes the effects of rotational diffusion, nematic potential, and flow on the orientational distribution of a system of rods. Both of these statistical theories are cast in terms of the orientational distribution function, $f(\theta, t)$, which represents the probability that an individual rod is oriented parallel to the polar angle θ at time t.

Although the Marrucci and Maffettone model was developed to describe bulk rheological phenomena, it can be subjected to direct experimental tests using monolayer films. In a recent paper, Schwiegk et al.[5] applied this model to their dichroism results for PcPS monolayers transferred to glass substrates. The 2D model was used to predict the orientational profile of the monolayer along the dipping direction of the substrate, since this orientation was thought to result from monolayer flow at the air−water interface. Although the actual surface flow induced by deposition was unknown, and the experiment was not able to access the dynamics of the flowing monolayer, reasonable agreement was obtained between the experimental results and the predictions of the theory.

We have modified the Marrucci and Maffettone model to describe the dynamics of polymer liquid crystal monolayers in extensional flow. This allows direct comparison with the *in situ* flow-dichroism results presented earlier. The governing equation for the orientational distribution function, f, can be written as

$$\frac{\partial f}{\partial t} = D\frac{\partial}{\partial \theta}\left[\frac{\partial f}{\partial \theta} + \frac{f}{kT}\frac{\partial V}{\partial \theta}\right] + \frac{\partial}{\partial \theta}(\dot{\epsilon} \sin 2\theta f) \qquad (6)$$

where D is the rotational diffusivity, kT is the thermal energy, V is the nematic potential, and $\dot{\epsilon}$ is the strain rate. Following Marrucci and Maffettone,[30] we developed a solution to this partial differential equation in terms of moments of the orientational distribution, e.g., $\langle\cos 2\theta\rangle$, $\langle\sin 2\theta\rangle$, $\langle\cos 4\theta\rangle$, $\langle\sin 4\theta\rangle$, where the brackets denote averages over the orientational distribution function, f. This procedure transforms eq 6 into an infinite series of coupled ordinary differential equations describing the dynamics of the moments. Marrucci and Maffettone found that truncation of the series after the fourth moment terms ($\langle\cos 4\theta\rangle$, $\langle\sin 4\theta\rangle$) through the use of a closure approximation provided an acceptable description of the shear flow behavior.[30] Using the same procedure, we have converted eq 6 into a set of four coupled ordinary differential equations; this introduces a single model parameter, m, into the equations for the fourth moment terms. The second moment of the distribution is of particular interest here, since it is linearly proportional to the dichroism and can thus be directly compared to our experimental results. The equation of motion for the second moment is given by

$$\frac{\partial\langle\cos 2\varphi\rangle}{\partial t} = -4D\langle\cos 2\varphi\rangle + 2DU\langle\cos 2\varphi\rangle(1 - \langle\cos 4\varphi\rangle) + \dot{\epsilon}[\langle\sin 4\varphi\rangle \sin 2\alpha + (1 - \langle\cos 4\varphi\rangle)\cos 2\alpha] \qquad (7)$$

where α is defined as the polar angle at which $\langle\sin 2\theta\rangle = 0$, and φ is the deviation of an individual polymer rod from this angle, $\varphi = \theta - \alpha$. For more details on this procedure, consult ref 30.

If the ratio of the strain rate to the rotational diffusivity is much greater than unit, the diffusive terms in the above model can be neglected ($D = 0$). This approximation would clearly be unsuitable for the PcPS Ultra/arachidyl alcohol system, due to the large orientational relaxation we observed at short times. For the PcPS Kurz/docosanoic acid system, however, the relaxation at short times was much weaker (not shown); therefore, we will compare this system with the predictions of the model in the limiting case of zero diffusivity. For initial conditions, we have taken $\langle\cos 2\varphi\rangle = 0.98$, $\langle\sin 4\varphi\rangle = 0$, and $\langle\cos 4\varphi\rangle = \langle\cos 2\varphi\rangle^2 = 0.96$.

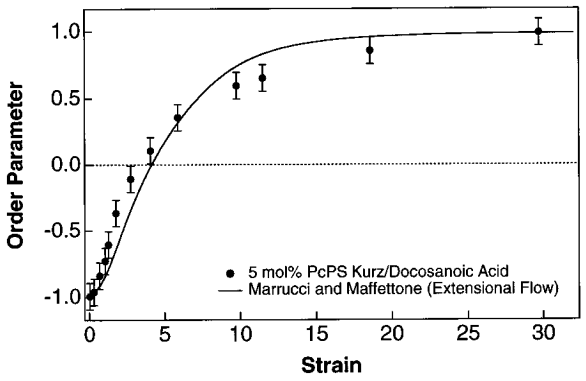

Figure 14. Comparison of observed flow-reversal dynamics (5 mol % PcPS Kurz/docosanoic acid) to the extensional flow predictions of the Marrucci and Maffettone model.

In Figure 14, the extensional flow model is compared to the observed flow-reversal dynamics for PcPS/docosanoic acid monolayers. Here, the data for the four strain rates have been averaged together to obtain a single principal curve. To allow direct comparison to the 2D model, the data have been normalized in terms of an order parameter. By plotting the experimental data in this manner, we have made the implicit assumption that the steady-state anisotropy corresponds to complete orientation of the polymer rods along the extension axis. As discussed earlier, this assumption is supported by the finding that the steady-state anisotropy is independent of strain rate for the rates investigated. The 2D model is in qualitative agreement with the flow-reversal dynamics for PcPS/docosanoic acid monolayers, predicting the observed sigmoidal shape of the response. We found that this qualitative shape is insensitive to the choice of the model parameter, m. The quantitative agreement is also excellent, but is based on favorable selection of the model parameter. The model also predicts strain scaling, in which the dynamics depend not on the strain rate *per se*, but on the product of strain rate and time. Future modeling efforts will include terms to describe the more interesting dynamics of the PcPS Ultra/arachidyl alcohol monolayers.

Summary

In summary, we performed *in situ* studies to investigate the influence of flow on molecular orientation in rodlike polymer monolayers at the air−water interface. Compression of a PcPS monolayer was found to align the PcPS molecules perpendicular to the compression direction. A four-roll mill was used to induce an extensional flow in the plane of the monolayer, and the orientational distribution of the polymer molecules was probed using high-speed optical techniques. On average, the PcPS molecules aligned parallel to the extension axis, indicating a strong association between flow and molecular orientation in this system. For 5 mol % PcPS Ultra/arachidyl alcohol monolayers, the degree of order at steady state was independent of strain rate

above 0.02 s^{-1}, suggesting complete alignment of the polymer backbones. On reversing the flow direction, the dynamics of the orientation process were found to scale with total strain, signifying the presence of a single time scale in the orientational response, namely the coupling of molecular orientation to the imposed flow. Following flow cessation, the monolayer undergoes partial relaxation but remains ordered at rest. In addition, the well-defined nature of the extensional flow allows the use of two-dimensional statistical models to simulate the observed flow dynamics. The methods employed in this paper provide important fundamental information regarding the influence of flow on polymer dynamics in constrained geometries. Although the present work takes advantage of the large optical absorption of PcPS to probe molecular orientation, the techniques are readily adapted to the more general case of materials with anisotropy in the real part of the refractive index (birefringence). Future work will include monolayer systems with more complex dynamics, and will also address the influence of an applied shear flow.

Acknowledgment. This work was supported in part by the NSF Materials Research Science and Engineering Program through the Center on Polymer Interfaces and Macromolecular Assemblies (CPIMA). The authors acknowledge The Fannie and John Hertz Foundation for fellowship support of M.C.F. In addition, we acknowledge funding from the Center for Materials Research at Stanford University, the AT&T Foundation, and the Polymer Program of the NSF. Finally, we thank Dr. Andreas Ferencz and Professor Gerhard Wegner of the Max Planck Institute for Polymer Research in Mainz for generous samples of PcPS.

References and Notes

(1) Roberts, G. G. *Langmuir−Blodgett Films*; Plenum: New York, 1990. Ulman, A. *An Introduction to Ultrathin Organic Films*; Academic Press: Boston, MA, 1991.
(2) Swalen, J. D.; Allara, D. L.; Andrade, J. D.; Chandross, E. A.; Garoff, S.; Israelachvili, J.; McCarthy, T. J.; Murry, R.; Pease, R. F.; Rabolt, J. F.; Wynne, K. J.; Yu, H. *Langmur* **1987**, *3*, 932.
(3) Duda, G.; Schouten, A. J.; Arndt, T.; Lieser, G.; Schmidt, G. F.; Bubeck, C.; Wegner, G. *Thin Solid Films* **1988**, *159*, 332.
(4) Orthmann, E.; Wegner, G. *Angew. Chem., Int. Ed. Engl.* **1986**, *25*, 1105.
(5) Schwiegk, S.; Vahlenkamp, T.; Xu, Y.; Wegner, G. *Macromolecules* **1992**, *25*, 2513.
(6) Embs, F. W.; Wegner, G.; Neher, D.; Albouy, P.; Miller, R. D.; Willson, C. G.; Schrepp, W. *Macromolecules* **1991**, *24*, 5068. Kani, R.; Yoshida, H.; Nakano, Y.; Murai, S.; Mori, Y.; Kawata, Y.; Hayase, S. *Langmuir* **1993**, *9*, 3045. Kani, R.; Nakano, Y.; Majima, Y.; Hayase, S.; Yuan, C. H.; West, R. *Macromolecules* **1994**, *27*, 1911. Seki, T.; Tamaki, T.; Ueno, K. *Thin Solid Films* **1994**, *243*, 625.
(7) Sorita, T.; Miyake, S.; Fujioka, H.; Nakajima, H. *Jpn. J. Appl. Phys.* **1991**, *30*, 131. Ito, S.; Kanno, K.; Ohmori, S.; Onogi, Y.; Yamamoto, M. *Macromolecules* **1991**, *24*, 659. Nishikata, Y.; Komatsu, K.; Kakimoto, M.; Imai, Y. *Thin Solid Films* **1992**, *210/211*, 29. Yang, X. M.; Gu, N.; Lu, Z. H.; Wei, Y. *Phys. Lett. A* **1993**, *183*, 111.
(8) Teerenstra, M. N.; Vorenkamp, E. J.; Schouten, A. J.; Nolte, R. J. M. *Thin Solid Films* **1991**, *196*, 153. Tsukruk, V. V.; Bliznyuk, V. N.; Reneker, D. H. *Thin Solid Films* **1994**, *244*, 745. Vandevyver, M., et al. *Langmuir* **1993**, *9*, 1561.
(9) Zasadzinski, J. A.; Viswanathan, R.; Madsen, L.; Garnaes, J.; Schwartz, D. K. *Science* **1994**, *263*, 1726. Shih, M. C.; Peng, J. B.; Huang, K. G.; Dutta, P. *Langmuir* **1993**, *9*, 776.
(10) Riegler, J. E. *Rev. Sci. Instrum.* **1988**, *59*, 2220. Riegler, H.; Spratte, K. *Thin Solid Films* **1992**, *210/211*, 9.
(11) Schwartz, D. K.; Knobler, C. M.; Bruinsma, R. *Phys. Rev. Lett.* **1994**, *73*, 2841.
(12) Benvegnu, D. J.; McConnell, H. M. *J. Phys. Chem.* **1992**, *96*, 6820. Stone, H. A.; McConnell, H. M. *Proc. R. Soc. London, Ser. A* **1995**, *448*, 97.
(13) Wegner, G. *Thin Solid Films* **1992**, *216*, 105.
(14) Fuller, G. G. *Annu. Rev. Fluid Mech.* **1990**, *22*, 387.
(15) Daniel, M. F.; Hart, J. T. T. *J. Mol. Electron.* **1985**, *1*, 97.
(16) Taylor, G. I. *Proc. R. Soc. London, Ser. A* **1934**, *146*, 501.
(17) Giesekus, H. *Rheol. Acta* **1962**, *2*, 113.
(18) Batchelor, G. K. *J. Fluid Mech.* **1971**, *46*, 813.
(19) Gupta, V. K.; Kornfield, J. A.; Ferencz, A.; Wegner, G. *Science* **1994**, *265*, 940.
(20) Higdon, J. J. L. *Phys. Fluids A* **1993**, *5*, 274.
(21) Malcolm, B. R. *J. Colloid Interface Sci.* **1985**, *104*, 520.
(22) Moldenaers, P.; Fuller, G. G.; Mewis, J. *Macromolecules* **1989**, *22*, 960.
(23) Batchelor, G. K. *An Introduction to Fluid Dynamics*; Cambridge University Press: New York, 1967.
(24) Miyano, K.; Hasegawa, T. *Thin Solid Films* **1991**, *205*, 117. Tomioka, Y.; Imazeki, S.; Tanaka, N. *Chem. Phys. Lett.* **1990**, *174*, 433. Nishikata, Y.; Komatsu, K.; Kakimoto, M.; Imai, Y. *Thin Solid Films* **1992**, *210/211*, 29.
(25) Larson, R. G. *Constitutive Equations for Polymer Melts and Solutions*; Butterworths: Boston, 1988.
(26) Odell, J. A.; Keller, A.; Atkins, E. D. T. *Macromolecules* **1985**, *18*, 1443. Cathey, C. Ph.D. Thesis, Stanford University, 1989.
(27) Srinivasarao, M.; Berry, G. C. *J. Rheol.* **1991**, *35*, 379.
(28) Marrucci, G.; Maffettone, P. L. *Macromolecules* **1989**, *22*, 4076.
(29) Doi, M. *J. Polym. Sci., Polym. Phys. Ed.* **1981**, *19*, 229.
(30) Maffettone, P. L.; Marrucci, G. *J. Non-Newtonian Fluid Mech.* **1991**, *387*, 273.

MA9507812